Supplemental Information

Supplemental Table 1. Primers used in qRT-PCR analyses.

Gene	Forward (5'to 3')	Reverse (5' to 3')
ARRB1	ggttcagtatgccccagaga	cgtcttgttggtgttgttgg
CBX5	atcgctcggggctttgagag	tgcaagaaccaggtcagcttc
CEACAM5	agattgcagtgagcccagat	ctgcttcatcttggtggaca
CYP1A1	catcccccacagcacaacaag	caggggtgagaaaccgttcag
CYP1B1	ctggatttggagaacgtaccg	tgatccaattctgcctgcact
DHRS3	gacgctttggatgtgcagta	atgatgatgccctcctcaag
GCNT1	cgcacacattttcaacaacc	gcagtctgggaaagactgagg
HPRT	cctcaggcgaacctctcggct	cagggctgcgggtcgccata
PPARG	ttcagaaatgccttgcagtg	ccaacagcttctccttctcg
RERG	acctaccgacaccaagcaac	cctcaaaacttcctcggtca
RGS16	caagacacgtctggggatct	caggtcgaacgactctctcc
SNAI2	tgctttggctttctggttct	tttgtttgtggtgcagtggt
TGBF2	gcatttcttcactccgaagc	tgaattccatgctcttgcag
CLDN6	cccttatctccttcgcagtg	atgctgttgcccgatgaaag
DNMT1	gaccatcaggcattctacc	ttacatttcccacactcagg
FKBP4	gggctcaagggatactcacac	cccaagctgagagtcggtc
GSTP1	caaatacatctccctcatctacac	ttgcctccctggttctgg
KIF1A	cccaagctgagagtctggtc	accagacccgatgtaactgc
MAL	ttttacctcaggcctcagt	acaccatctgggttttcagc
PHD3	gggcaaatactacgtcaaggag	agtcttcagtgagggcagattc
P16	gcgatgtcgcacggtacctg	gggcagttgtggccctgtag
TFPI-2	gggcctacttctccgttac	cacactggtcgtccacactc
VGF	acccgagtgaatctggagag	gacactccttccccgaactt

Supplemental Table 2. Effect of anthraquinone compounds on Dnmt1 activity. The observed initial velocity in the presence of 10 µM compound. Assays included 10 nM oligonucleotide 8006, 10 µM AdoMet and 2 nM Dnmt1 (621-1600). None of these anthraquinones (ChemBridge Corp., San Diego, CA) had an effect on Dnmt1 activity.

Compound	Initial Velocity (RFU/min)
DMSO Control	47 ± 4
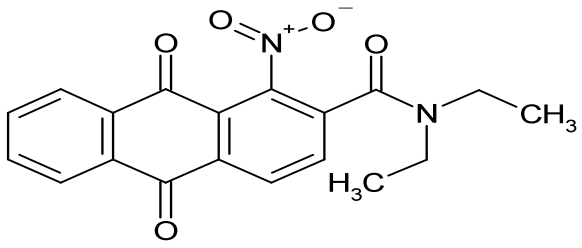 UI1055	48 ± 6
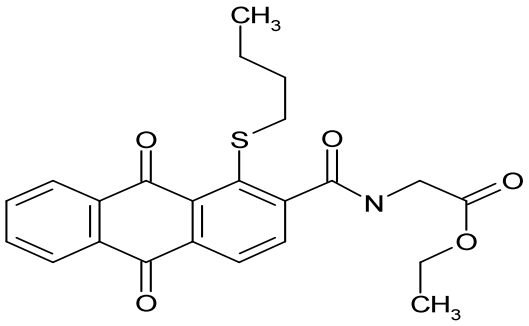 UI1060	48 ± 5
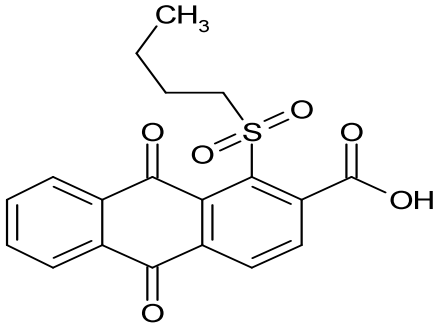 UI1061	50 ± 5

Supplemental Table 3. Changes in gene expression caused by laccaic acid A in MCF-7 cells.

Gene Symbol	RefSeq	Fold Change	p-value
CYP1A1	AM233518	13.47	3.4E-05
RGS16	AF493937	4.86	3.2E-04
UGT2B1	--	4.59	5.2E-04
TARP	--	4.57	1.4E-04
HEY2	AB044755	4.34	1.6E-03
BMPR1B	AK299930	4.16	1.3E-04
CEACAM6	BT009774	4.07	5.3E-03
FAM105A	--	3.96	2.3E-05
CEACAM5	BC034671	3.24	1.2E-03
MICAL2	AB110785	3.22	5.8E-05
NECAB1	BC016340	3.18	4.9E-04
UGT2B15	AK289419	2.98	1.7E-03
PPFIA2	AF034799	2.79	1.5E-03
PMP22	--	2.59	8.9E-04
DHRS3	ENST00000376223	2.42	7.8E-04
ELOVL3	BC034344	2.37	8.8E-04
GCNT1	AJ420416	2.33	3.0E-04
LAMA3	AK096422	2.33	5.6E-04
C1QTNF9B	BC110413	2.32	4.2E-03
RERG	AF339750	2.30	5.0E-03
ARRB1	AF084040	2.29	4.9E-05
PPARG	ENST00000397010	2.28	6.5E-03
NPY1R	AK296624	2.28	1.5E-02
CYP1B1	AK303862	2.26	1.9E-05
SELL	AK298705	2.25	7.8E-05
FAM46C	BC036516	2.25	9.4E-04
BPIFB1	AF364078	2.23	2.5E-03
WLS	AB097018	2.23	3.5E-03
LMO3	AB044745	2.22	4.2E-04
ALDH1A3	BC069274	2.16	6.8E-03
TSPAN2	GU971730	2.16	1.1E-03
TNFSF10	AK296085	2.06	6.2E-04
MBOAT1	AK296857	2.05	2.4E-04
GLDN	AY358144	2.02	2.0E-03
LMCD1	AF216709	2.01	2.7E-03
SGMS2	AK290344	-2.01	1.8E-05
CACNG4	AF162692	-2.04	1.5E-03
NT5E	BC065937	-2.04	1.4E-03
CRISP3	AK292786	-2.04	2.9E-03
ABCA12	AF418105	-2.05	2.9E-04
MAP3K1	--	-2.05	1.9E-05
B3GNT5	AB045278	-2.11	7.3E-04
ITGB6	AK290300	-2.11	1.7E-03
TGM2	S81734	-2.16	5.9E-03

EFEMP1	AK290599	-2.18	6.3E-04
DIO2	AB041843	-2.21	1.5E-02
ST3GAL5	AB018356	-2.35	1.9E-03
MALL	BC003179	-2.36	1.4E-03
KIAA1324	AK297221	-2.39	9.9E-05
ID3	AK290003	-2.47	8.0E-05
PCSK2	AK294200	-2.49	1.6E-03
CAV1	AK290871	-2.54	2.2E-03
MME	AK291761	-2.60	2.2E-04
KRT80	BC065180	-2.62	4.8E-04
IFI27	AK289535	-2.62	5.7E-03
EDN1	AK291838	-2.65	1.4E-03
MGP	ENST00000539261	-2.81	3.1E-03
CLDN1	AF086514	-2.81	2.7E-03
ANXA1	BC001275	-2.88	4.5E-03
SNAI2	BC014890	-3.27	2.6E-04
SERPINA3	--	-3.76	4.1E-04
ID1	AK291152	-4.33	1.9E-04
ID2	AY634687	-4.57	9.6E-05
TGFB2	AK295671	-6.10	4.6E-05

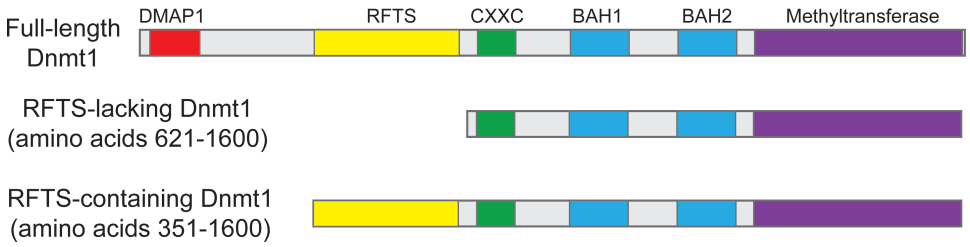

Figure S1. Domain structure of full-length and truncated Dnmt1 proteins. Full-length Dnmt1 consists of a large N-terminal regulatory region (~1100 amino acids) that is comprised of several small globular domains and a C-terminal catalytic methyltransferase domain. Both RFTS-lacking and RFTS-containing Dnmt1 are used in *in vitro* experiments to investigate inhibition of Dnmt1.

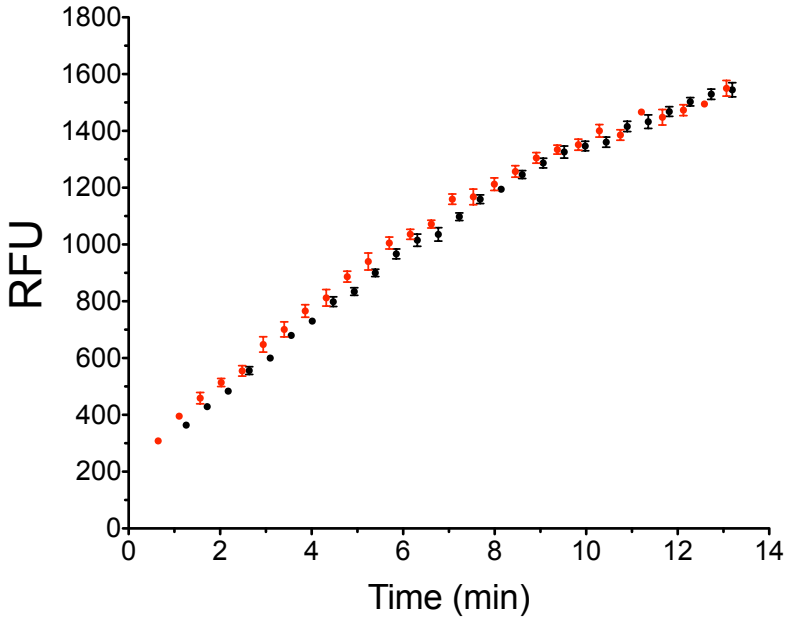

Figure S2. Effect of LCA on Gla I activity. Gla I activity was measured using an internally quenched hairpin DNA with a fully methylated GCGC site (the cleavage site of Gla I). Gla I cleavage of the oligonucleotide releases the 5' fluorophore from the 3' quencher, generating fluorescence in real-time. The time-dependent cleavage of 8 nM oligonucleotide substrate with 0.4 U of enzyme in the presence of 0 LCA (black) or 10 μM LCA (red). Addition of LCA has no effect on the activity of Gla I.

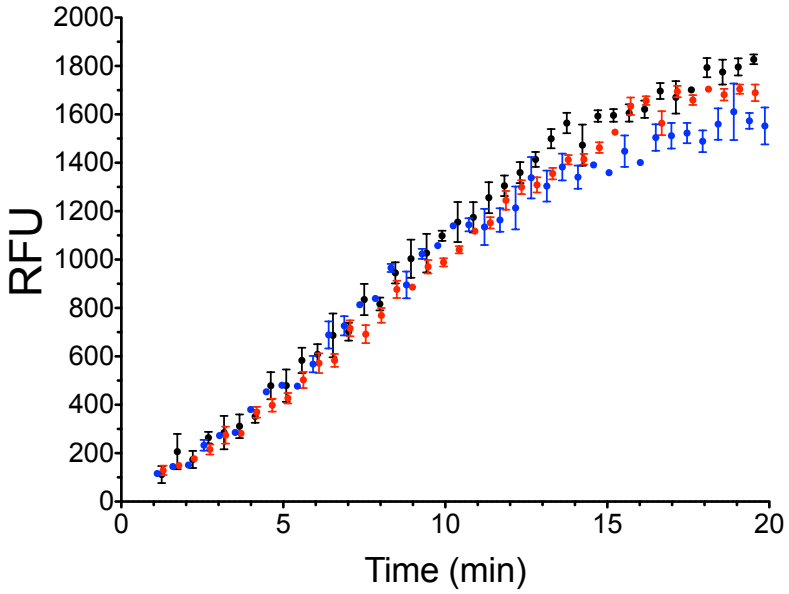

Figure S3. Effect of control anthraquinones on Dnmt1 activity. Dnmt1 activity was measured using the Gla I-coupled DNA methylation assay. Assays containing 20 nM oligonucleotide 8006, 10 µM AdoMet, and 50 µM anthraquinone were conducted using 2 nM Dnmt1 (621-1600). Addition of anthraquinone (red) or anthraquinone 2-carboxylic acid (blue) had no effect on the observed activity of Dnmt1. The DMSO control assay is shown in black.

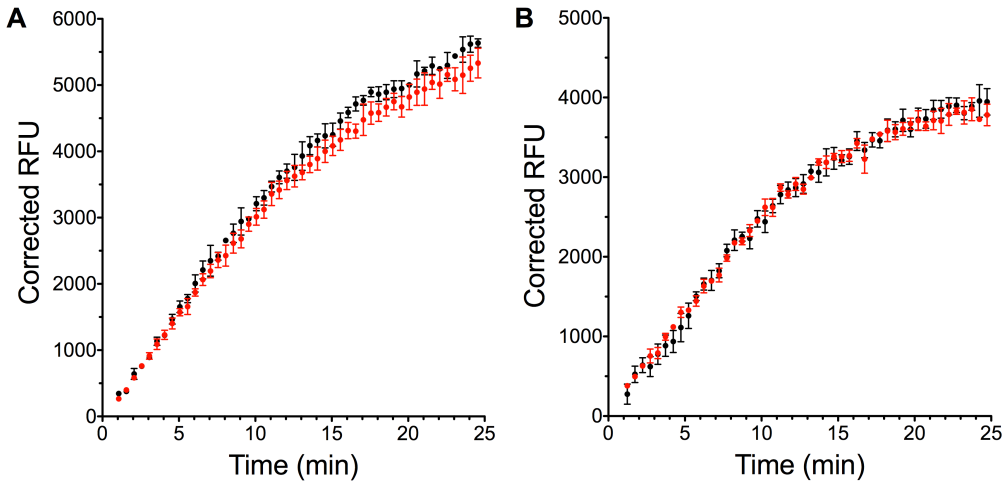

Figure S4. Effect of LCA pre-incubation on Dnmt1 activity. 5 μM LCA was incubated with either Dnmt1 (0.5 μM) or Dnmt1 and AdoMet (0.5 μM and 50 μM respectively) for 30 minutes. Enzyme was then buffer exchanged into assay buffer lacking LCA and DNA substrate and used to initiate DNA methylation assays. Assays containing 20 nM oligonucleotide 8006 and 20 μM AdoMet were conducted using 1.5 nM (A) or 1 nM (B) buffer exchanged Dnmt1 (621-1600). Panel A shows Dnmt1 incubated with LCA, while panel B shows Dnmt1 and SAM incubated LCA. In both cases, incubation with LCA (red) had no effect on the observed activity of Dnmt1. The DMSO control assay is shown in black.

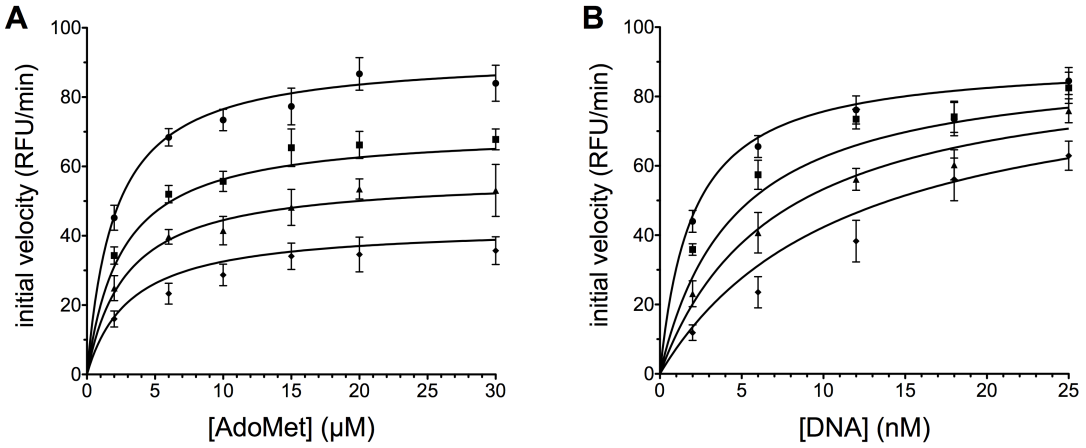

Figure S5. Mode of inhibition of LCA. A) AdoMet-dependent LCA inhibition kinetics. LCA was used as an inhibitor in reactions containing 20 nM DNA and varying concentrations of AdoMet (2-30 μM). Initial velocities ± SEM are shown for no LCA (●), 0.4 μM LCA (■), 0.8 μM LCA (▲) and 1.5 μM LCA (◆). The same data are shown as a double reciprocal plot in Fig 4B. LCA exhibits mixed inhibition with respect to AdoMet, indicating that LCA binds both the free enzyme and the enzyme•SAM complex. The data were fit to the mixed model inhibition expression in Prism giving a $K_{m,AdoMet}$ of 2.0 ± 0.2 μM, $K_{i,a}$ of 640 ± 200 nM, $K_{i,b}$ of 1.4 ± 0.4 μM and V_{max} of 92 ± 2 RFU/min. B) DNA-dependent LCA inhibition kinetics. LCA was used as an inhibitor in reactions containing 30 μM AdoMet and varying concentrations of DNA (2-25 nM). Initial velocities ± SEM are shown for no LCA (●), 0.4 μM LCA (■), 0.8 μM LCA (▲) and 1.5 μM LCA (◆). The same data are shown as a double reciprocal plot in Fig 4C and indicates LCA is competitive with DNA substrate. Globally fitting these data to the competitive inhibition equation in Prism gives a $K_{m,DNA}$ of 1.9 ± 0.4 nM, K_i of 310 ± 80 nM and V_{max} of 91 ± 4 RFU/min.